Chapter 4
Drug Release

An equation relating the rate of release of solid drugs suspended in ointment bases into perfect sinks is derived. . . . The amount of drug released . . . is proportional to the square root of time.

Takeru Higuchi
School of Pharmacy, University of Wisconsin, Madison
Journal of Pharmaceutical Sciences 50:874–875 (1961)

The term "release" encompasses several processes that contribute to the transfer of drug from the dosage form to the bathing solution (e.g., gastrointestinal fluids, dissolution medium). The objective of this chapter is to present the spectrum of mathematical models that have been developed to describe drug release from controlled-release dosage forms. These devices are designed to deliver the drug at a rate that is governed more by the dosage form and less by drug properties and conditions prevailing in the surrounding environment. The release mechanism is an important factor in determining whether both of these objectives can be achieved. Depending on the release mechanism, the controlled-release systems can be classified into

1. diffusion-controlled,
2. chemically controlled, and
3. swelling-controlled.

By far, diffusion is the principal release mechanism, since apart from the diffusion-controlled systems, diffusion takes place at varying degrees in both chemically and swelling-controlled systems. The mathematical modeling of release from diffusion-controlled systems relies on the fundamental Fick's law (2.11), (2.16) with either concentration-independent or concentration-dependent diffusion coefficients. Depending on the formulation characteristics of the device, various types of diffusion can be conceived, i.e., diffusion through an inert matrix, a hydrogel, or a membrane. For chemically controlled systems, the rate of drug release is controlled by

- the degradation and in some cases the dissolution of the polymer in erodible systems or

P. Macheras, A. Iliadis, *Modeling in Biopharmaceutics, Pharmacokinetics and Pharmacodynamics*, Interdisciplinary Applied Mathematics 30,
DOI 10.1007/978-3-319-27598-7_4

- the rate of the hydrolytic or enzymatic cleavage of the drug–polymer chemical bond in pendant chain systems.

For swelling-controlled systems the swelling of the polymer matrix after the inward flux of the liquid bathing the system induces the diffusion of drug molecules toward the bathing solution.

In the following sections of this chapter we present the mathematical models used to describe drug release from hydroxypropyl methylcellulose (HPMC) controlled-release dosage forms. HPMC is the most widely used hydrophilic polymer for oral drug delivery systems. Since HPMC exhibits high swellability, drug release from HPMC-based systems is the result of different simultaneously operating phenomena. In addition, different types of HPMC are commercially available and therefore a universal pattern of drug release from HPMC-based systems cannot be pointed out. Accordingly, a wide spectrum of models has been used to describe drug release kinetics from HPMC-based matrix tablets. The sequential presentation below of the mathematical models presented attempts to provide hints to their interrelationships, along with their time evolution, and avoids a strict classification, e.g., empirical vs. mechanistically based models. The last part of the chapter is devoted to the rapidly emerging applications of Monte Carlo simulation in drug release studies. Finally, a brief mention of applications of nonlinear dynamics to drug release phenomena is made at the end of the chapter.

4.1 The Higuchi Model

In 1961 Higuchi [57] analyzed the kinetics of drug release from an ointment assuming that the drug is homogeneously dispersed in the planar matrix and the medium into which drug is released acts as a perfect sink, Figure 4.1. Under these pseudo-steady-state conditions, Higuchi derived (4.1) for the cumulative amount $q(t)$ of drug released at time t:

$$q(t) = \mathcal{A}\sqrt{\mathcal{D}(2c_0 - c_s)c_s t}, \quad c_0 > c_s, \tag{4.1}$$

where $\mathcal{A}$ is the surface area of the ointment exposed to the absorbing surface, $\mathcal{D}$ is the diffusion coefficient of drug in the matrix medium, and c_0 and c_s are the initial drug concentration and the solubility of the drug in the matrix, respectively. Although a planar matrix system was postulated in the original analysis [57], modified forms of (4.1) were published [58–60] for different geometries and matrix characteristics, e.g., granular matrices.

Equation (4.1) is frequently written in simplified form:

$$\frac{q(t)}{q_\infty} = k\sqrt{t}, \tag{4.2}$$

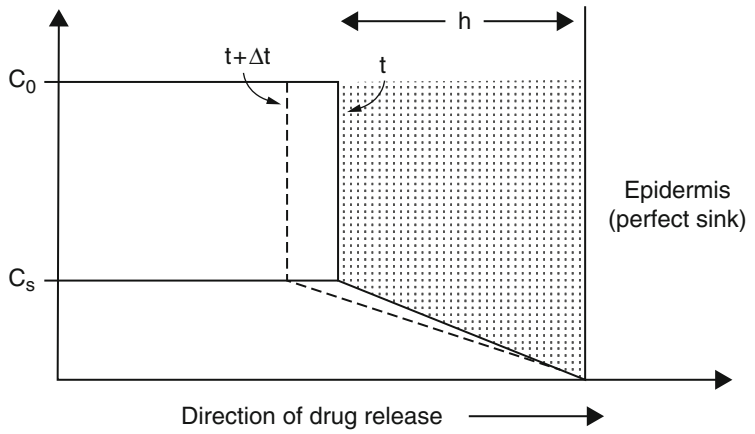

Fig. 4.1 The spatial concentration profile of drug (*solid line*) existing in the ointment containing the suspended drug in contact with a perfect sink according to Higuchi's assumptions. The broken line indicates the temporal evolution of the profile, i.e., a snapshot after a time interval Δt. For the distance h above the exposed area, the concentration gradient $(c_0 - c_s)$ is considered constant assuming that c_0 is much higher than c_s

where q_∞ is the cumulative amount of drug released at infinite time and k is a composite constant with dimension time$^{-1/2}$ related to the drug diffusional properties in the matrix as well as the design characteristics of the system. For a detailed discussion of the assumptions of the Higuchi derivation in relation to a valid application of (4.2) to real data, the reader can refer to the review of Siepmann and Peppas [61].

Equation (4.2) reveals that the fraction of drug released is linearly related to the square root of time. However, (4.2) cannot be applied throughout the release process since the assumptions used for its derivation are not obviously valid for the entire release course. Additional theoretical evidence for the time limitations in the applicability of (4.2) has been obtained [62] from an exact solution of Fick's second law of diffusion for thin films of thickness δ under perfect sink conditions, uniform initial drug concentration with $c_0 > c_s$, and assuming constant diffusion coefficient of drug $\mathcal{D}$ in the polymeric film. In fact, the short-time approximation of the exact solution is

$$\frac{q(t)}{q_\infty} = 4\sqrt{\frac{\mathcal{D}t}{\pi\delta^2}} = k'\sqrt{t}, \tag{4.3}$$

where $k' = 4\sqrt{\mathcal{D}/\pi\delta^2}$. Again, the proportionality between the fraction of drug released and the square root of time is justified (4.3). These observations have led to a rule of thumb, which states that the use of (4.2) for the analysis of release data is recommended only for the first 60% of the release curve $(q(t)/q_\infty \leq 0.60)$. This arbitrary recommendation does not rely on strict theoretical and experimental

findings and is based only on the fact that completely different physical conditions have been postulated for the derivation of the equivalent (4.2) and (4.3), while the underlying mechanism in both situations is classical diffusion. In this context, a linear plot of the cumulative amount of drug released $q(t)$ or the fraction of drug released $q(t)/q_\infty$ (utilizing data up to 60% of the release curve) vs. the square root of time is routinely used in the literature as an indicator for diffusion-controlled drug release from a plethora of delivery systems.

In 2011, an issue of the International Journal of Pharmaceutics (Vol. 418, No. 1, pp. 1–148, 10 October 2011) entitled "Mathematical modeling of drug delivery systems: Fifty years after Takeru Higuchi's models" was published commemorating the 50-th anniversary of the Higuchi's publication [57].

4.2 Systems with Different Geometries

One of the first physicochemical studies [63] dealing with diffusion in glassy polymers published in 1968 can be considered as the initiator of the realization that two apparently independent mechanisms of transport, a Fickian diffusion and a Case II transport, contribute in most cases to the overall drug release. Fick's law governs the former mechanism, while the latter reflects the influence of polymer relaxation on the molecules' movement in the matrix [64]. The first studies on this topic [65, 66] were focused on the analysis of Fickian and non-Fickian diffusion as well as the coupling of relaxation and diffusion in glassy polymers. The models used to describe drug release from different geometries are quoted below:

1. Fickian diffusional release from a thin polymer film. Equation (4.3) gives the short-time approximation of the fractional drug released from a thin film of thickness δ.
2. Case II release from a thin polymer film. The fractional drug release $q(t)/q_\infty$ follows zero-order kinetics [67, 68] according to

$$\frac{q(t)}{q_\infty} = \frac{2k_0}{c_0\delta}t, \tag{4.4}$$

   where k_0 is the Case II relaxation constant and c_0 is the drug concentration, which is considered uniform.
3. Case II radial release from a cylinder. The following equation describes the fractional drug released, $q(t)/q_\infty$, when Case II drug transport with radial release from a cylinder of radius ρ is considered [68]:

$$\frac{q(t)}{q_\infty} = \frac{2k_0}{c_0\rho}t - \left(\frac{k_0}{c_0\rho}t\right)^2. \tag{4.5}$$

4. Case II one-dimensional radial release from a sphere. For a sphere of radius ρ with Case II one-dimensional radial release, the fractional drug released, $q(t)/q_\infty$, is given [68] by

$$\frac{q(t)}{q_\infty} = \frac{3k_0}{c_0\rho}t - 3\left(\frac{k_0}{c_0\rho}t\right)^2 + \left(\frac{k_0}{c_0\rho}t\right)^3. \tag{4.6}$$

5. Case II radial and axial release from a cylinder. We quote below a detailed analysis of Case II radial and axial release from a cylinder [69] since (4.4) and (4.5) are special cases of the general equation derived in this section.

The analysis of Case II drug transport with axial and radial release from the cylinder depicted in Figure 4.2 is based on two assumptions:

- a boundary is formed between the glassy and rubbery phases of the polymer, and
- the movement of this boundary takes place under constant velocity.

First, the release surface is determined. A cylinder of height $2L$ that is allowed to release from all sides can be treated as a cylinder of height L that can release from the round side and the top only, Figure 4.2. This second case is easier to analyze and is also implied in [68] for the release of drug from a thin film of thickness $L'/2$. If the big cylinder of Figure 4.2 is cut in half across the horizontal line, two equal cylinders, each of height L, are formed. If drug release from the two newly formed areas (top and bottom) of the two small cylinders is not considered, the two cylinders of height L' exhibit the same release behavior as the big cylinder, i.e., $q(t)_{2L} = 2q(t)_L$ and $q_{\infty,2L} = 2q_{\infty,L}$; consequently,

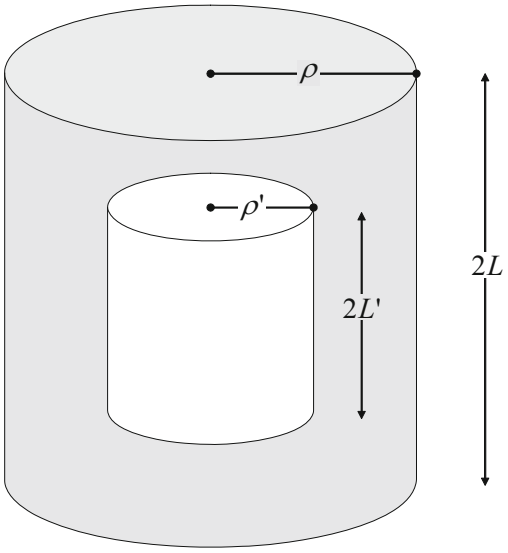

Fig. 4.2 Case II drug transport with axial and radial release from a cylinder of height $2L$ and radius ρ at $t = 0$. Drug release takes place from all sides of the big cylinder. The drug mass is contained in the gray region. After time t the height of the cylinder is reduced to $2L'$ and its radius to ρ' (*small cylinder*)

$$\frac{q(t)_{2L}}{q_{\infty,2L}} = \frac{q(t)_L}{q_{\infty,L}}.$$

This proportionality demonstrates that the analysis of the release results can describe both of the following cases: either a cylinder of height L that releases from the round and top surfaces or a cylinder of height $2L$ that releases from all sides, Figure 4.2.

At zero time, the height and radius of the cylinder are L and ρ, respectively, Figure 4.2. After time t the height of the cylinder decreases to L' and its radius to ρ' assuming Case II drug transport for both axial and radial release. The decrease rate of radius ρ' and height L' of the cylinder can be written

$$\dot{\rho}' = \dot{L}' = -\frac{k_0}{c_0}, \tag{4.7}$$

where k_0 is the Case II relaxation constant and c_0 is the drug concentration (considered uniform). The assumed value of the penetration layer speed is implied from the analysis of the cases studied in [67, 68], which are simpler than the present case. Initial conditions for the above equations are simply $\rho'(0) = \rho$ and $L'(0) = L$.

After integration of (4.7), we obtain the following equations as well as the time for which each one is operating:

$$\begin{aligned} \rho' &= \rho - (k_0/c_0)\, t, \quad t \le (c_0/k_0)\, \rho, \\ L' &= L - (k_0/c_0)\, t, \quad t \le (c_0/k_0)\, L. \end{aligned} \tag{4.8}$$

This means that the smaller dimension of the cylinder (ρ or L) determines the duration of the phenomenon.

The amount of drug released at any time t is given by the following mass balance equation:

$$q(t) = c_0 \pi \left(\rho^2 L - \rho'^2 L'\right). \tag{4.9}$$

Substituting (4.8) into (4.9), the following expression for mass $q(t)$ as a function of time t is obtained:

$$q(t) = c_0 \pi \left[\rho^2 L - \left(\rho - \frac{k_0}{c_0} t\right)^2 \left(L - \frac{k_0}{c_0} t\right)\right].$$

And for the mass released at infinite time, we can write

$$q_\infty = c_0 \pi \rho^2 L.$$

From the previous equations, the fraction released $q(t)/q_\infty$ as a function of time t is obtained:

$$\frac{q(t)}{q_\infty} = \left(\frac{2k_0}{c_0\rho} + \frac{k_0}{c_0 L}\right)t - \left(\frac{k_0^2}{c_0^2\rho^2} + \frac{2k_0^2}{c_0^2\rho L}\right)t^2 + \frac{k_0^3}{c_0^3\rho^2 L}t^3. \tag{4.10}$$

This equation describes the entire fractional release curve for Case II drug transport with axial and radial release from a cylinder. Again, (4.10) indicates that the smaller dimension of the cylinder (ρ or L) determines the total duration of the phenomenon. When $\rho \gg L$, (4.10) can be approximated by

$$\frac{q(t)}{q_\infty} = \frac{k_0}{c_0 L}t,$$

which is identical to (4.4) with the difference of a factor of 2 due to the fact that the height of the cylinder is $2L$. When $\rho \ll L$, (4.10) can be approximated by

$$\frac{q(t)}{q_\infty} = \frac{2k_0}{c_0\rho}t - \left(\frac{k_0}{c_0\rho}t\right)^2,$$

which is also identical to (4.5). These results demonstrate that the previously obtained (4.4) and (4.5) are special cases of the general solution (4.10).

4.3 The Power-Law Model

Peppas and coworkers [66, 70] introduced a semiempirical equation (the so-called power law) to describe drug release from polymeric devices in a generalized way:

$$\frac{q(t)}{q_\infty} = kt^\lambda, \tag{4.11}$$

where k is a constant reflecting the structural and geometric characteristics of the delivery system expressed in dimensions of time$^{-\lambda}$, and λ is a release exponent the value of which is related to the underlying mechanism(s) of drug release. Equation (4.11) enjoys a wide applicability in the analysis of drug release studies and the elucidation of the underlying release mechanisms. Apart from its simplicity, the extensive use of (4.11) is mainly due to the following characteristics:

- Both Higuchi equations (4.1) and (4.3), which describe Fickian diffusional release from a thin polymer film, are special cases of (4.11) for $\lambda = 0.5$; also, (4.4) is a special case of (4.11) for $\lambda = 1$.
- It can describe adequately the first 60% of the release curve when (4.5) and (4.6) govern the release kinetics [68, 69].
- The value of the exponent λ obtained from the fitting of (4.11) to the first 60% of the experimental release data, from polymeric-controlled delivery systems of different geometries, is indicative of the release mechanism, Table 4.1.

Table 4.1 Values of the exponent λ in (4.11) and the corresponding release mechanisms from polymeric-controlled delivery systems of various geometries [65].

Exponent λ			**Release**
Thin film	Cylinder	Sphere	**mechanism**
0.5	0.45	0.43	Fickian diffusion
$0.5 < \lambda < 1.0$	$0.45 < \lambda < 0.89$	$0.43 < \lambda < 0.85$	Anomalous transport
1.0	0.89	0.85	Case II transport

From the values of λ listed in Table 4.1, only the two extreme values 0.5 and 1.0 for thin films (or slabs) have a physical meaning. When $\lambda = 0.5$, pure Fickian diffusion operates and results in diffusion-controlled drug release. It should be recalled here that the derivation of the relevant (4.3) relies on short-time approximations and therefore the Fickian release is not maintained throughout the release process. When $\lambda = 1.0$, zero-order kinetics (Case II transport) are justified in accord with (4.4). Finally, the intermediate values of λ (cf. the inequalities in Table 4.1) indicate a combination of Fickian diffusion and Case II transport, which is usually called *anomalous transport*.

It is interesting to note that even the more realistic model adhering to the Case II radial and axial drug release from a cylinder (4.10) can be described by the power-law equation. In this case, pure Case II drug transport and release is approximated (Table 4.1) by the following equation:

$$\frac{q(t)}{q_\infty} \approx kt^{0.89}. \tag{4.12}$$

A typical example of comparison between (4.10) and (4.12) when $\rho < L$ is shown in Figure 4.3. One should note the resemblance, along the first 60% of the curves, to the kinetic profiles derived from these equations.

4.3.1 Higuchi Model vs. Power-Law Model

Drug release data are frequently plotted as percent (or fractional) drug released vs. $t^{1/2}$. This type of plot is usually accompanied by linear regression analysis using $q(t)/q_\infty$ as dependent and $t^{1/2}$ as independent variable. This routinely applied procedure can lead to misinterpretations regarding the diffusional mechanism, as is shown below using simulation studies [71].

Simulated data were generated from (4.11) using values for λ and k ranging from 0.4 to 0.65 and from 0.05 to 0.5, respectively. The range of λ values is the neighborhood of the Higuchi exponent 0.5, which is the theoretical value for a diffusion-controlled release process. Moreover, values of λ in the range $0.4 - 0.65$ are frequently quoted in the literature for the discernment of drug release mechanisms (pure diffusion, anomalous transport, and combination) from HPMC matrix devices of different geometries [67, 68]. The values assigned to k are similar

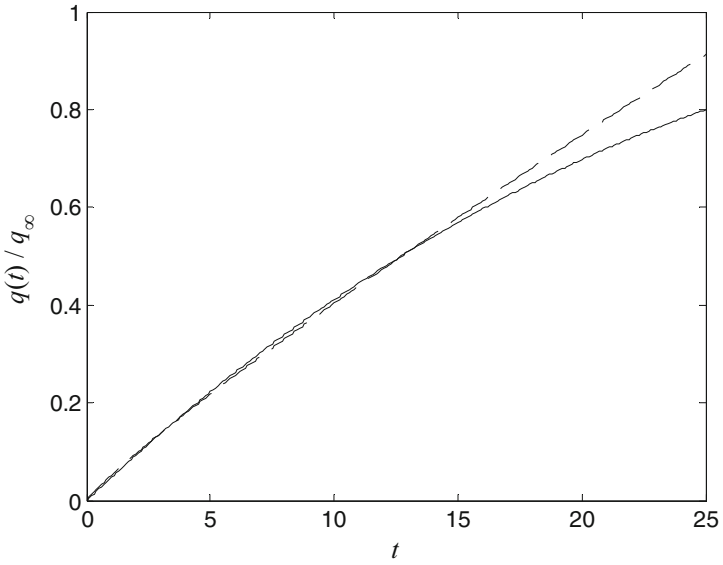

Fig. 4.3 Fractional drug release $q\,(t)\,/q_\infty$ vs. time (arbitrary units) for Case II transport with axial and radial release from a cylinder. Comparison of the solutions presented by (4.10) with $k_0 = 0.01$, $c_0 = 0.5$, $\rho = 1$, $L = 2.5$ (*dashed line*) and (4.12) with $k = 0.052$ (*solid line*)

to the estimates obtained when (4.3) is fitted to drug release data, whereas k has dimension of time$^{-1/2}$. The constraint $q\,(t)\,/q_\infty \leq 1$ was used for each set generated from (4.11). The duration of the simulated release experiment was arbitrarily set equal to 8 ($t \leq 8$). Therefore, the number of the simulated data generated from (4.11) varied according to the specific value assigned to k using in all cases a constant time step, 0.01. The pairs of data $(q\,(t)\,/q_\infty, t)$ generated from (4.11) were further analyzed using linear regression analysis in accord with (4.3).

Table 4.2 shows the results of linear regression analysis ($q\,(t)\,/q_\infty$ vs. $t^{1/2}$) for the data generated from (4.11). As expected, the theoretically correct sets of data ($\lambda = 0.5$) exhibited ideal behavior (intercept$= 0$, $R^2 = 1$). Judging from the determination coefficient R^2 values in conjunction with the number of data points utilized in regression, all other sets of data with $\lambda \neq 0.5$ are also described nicely if one does not apply a more rigorous analysis, e.g., plot of residuals. It is also worthy of mention that the positive intercepts were very close to zero and only in two cases ($k = 0.4, \lambda = 0.4$; $k = 0.5, \lambda = 0.4$) were they found to be in the range $0.10-0.11$. In parallel, any negative intercepts were very close to the origin of the axes.

These observations indicate that almost the entire set of data listed in Table 4.2 and generated from (4.11) can be misinterpreted as obeying (4.3). Under real experimental conditions the discernment of kinetics is even more difficult when linear regression of $q\,(t)\,/q_\infty$ vs. $t^{1/2}$ is applied. This is so if one takes into account

Table 4.2 Results of linear regression $q(t)/q_\infty$ vs. $t^{1/2}$ for data generated from (4.11). (a) Estimates not statistically significant different from zero were obtained. (b) Number of data points utilized in regression.

k	λ	Intercept	Slope	R^2	N^b
0.05	0.40	0.01287	0.03668	0.9970	800
	0.45	0.006719	0.04305	0.9993	800
	0.50	0^a	0.05	1	800
	0.55	−0.00576	0.05760	0.9994	800
	0.60	−0.01545	0.06571	0.9976	800
	0.65	−0.02436	0.07501	0.9950	800
0.30	0.40	0.0772	0.02201	0.9970	800
	0.45	0.04031	0.2583	0.9993	800
	0.50	0^a	0.3	1	800
	0.55	−0.04418	0.3456	0.9994	800
	0.60	−0.08866	0.3925	0.9976	743
	0.65	−0.1258	0.4349	0.9949	637
0.40	0.40	0.1030	0.2935	0.9970	800
	0.45	0.05270	0.3451	0.9993	766
	0.50	0^a	0.4	1	625
	0.55	−0.04676	0.4513	0.9994	529
	0.60	−0.08829	0.4987	0.9976	460
	0.65	−0.1253	0.5422	0.9948	4409
0.50	0.40	0.1117	0.3800	0.9969	565
	0.45	0.05243	0.4424	0.9993	466
	0.50	0^a	0.5	1	400
	0.55	−0.04649	0.5525	0.9993	352
	0.60	−0.0878	0.6002	0.9975	317
	0.65	−0.1245	0.6432	0.9947	290

- the usually small number of experimental data points available,
- the constraint for the percentage of drug released, $q\,(t)\,/q_\infty \leq 0.60$,
- the experimental error of data points,
- the high variability or lack of data points at the early stages of the experiment, and
- the possible presence of a delay in time.

Therefore, it is advisable to fit (4.11) directly to experimental data using nonlinear regression. Conclusions concerning the release mechanisms can be based on the estimates for λ and the regression line statistics [71].

4.4 Recent Mechanistic Models

Although the empirical and semiempirical models described above provide adequate information for the drug release mechanism(s), better insight into the release process can be gained from mechanistic models. These models have the advantage of being

more accurate and predictive. However, mechanistic models are more physically realistic and therefore mathematically more complex since they describe all concurrent physicochemical processes, e.g., diffusion, dissolution, swelling. Additionally, they require the use of time- and/or position-, direction-dependent diffusivities. This mathematical complexity is the main disadvantage of the mechanistic models since explicit analytical solutions of the partial differential equations cannot be derived. In this case, one has to rely on numerical solutions and less frequently on implicit analytical solutions.

Although the emphasis of this section will be on the most recent mechanistic approaches, the work of Fu et al. [72] published in 1976 should be mentioned since it deals with the fundamental release problem of a drug homogeneously distributed in a cylinder. In reality, Fu et al. [72] solved Fick's second law equation assuming constant cylindrical geometry and no interaction between drug molecules. These characteristics imply a constant diffusion coefficient in all three dimensions throughout the release process. Their basic result in the form of an analytical solution is

$$\frac{q(t)}{q_\infty} = 1 - \frac{8}{h^2\rho^2}\left[\sum_{i=1}^{\infty}\alpha_i^{-2}\exp\left(-\mathcal{D}\alpha_i^2 t\right)\right]\left[\sum_{j=1}^{\infty}\beta_j^{-2}\exp\left(-\mathcal{D}\beta_j^2 t\right)\right],$$

where $\beta_j = (2j+1)\,\pi/(2h)$, α_i are the roots of the equation $J_0(\rho\alpha) = 0$, and J_0 is the zero-order Bessel function. Here, h denotes the half-length, ρ the radius of the cylinder, and i and j are integers. Note that for small t the series is very slowly converging. Even keeping 100 terms of the above series is still not a good enough approximation of $q(t)/q_\infty$, for $t \approx 0$. For long times all terms with high values of α and β decay rapidly and only the term with the lowest value survives. The series reduces to a simple exponential after some time.

Gao et al. [73, 74] developed a mathematical model to describe the effect of formulation composition on the drug release rate for HPMC-based tablets. An effective drug diffusion coefficient $\mathcal{D}'$ was found to control the rate of release as derived from a steady-state approximation of Fick's law in one dimension:

$$\frac{q(t)}{q_\infty} = \frac{\mathcal{A}}{V}\sqrt{\frac{\mathcal{D}'t}{\pi}},$$

where $\mathcal{A}$ is the surface area and V the volume available for release, while $\mathcal{D}'$ corresponds to the quotient $\mathcal{D}/\tau$, where $\mathcal{D}$ is the classical drug diffusion coefficient in the release medium and τ is the tortuosity of the diffusing matrix.

In a series of papers Narasimhan and Peppas [75–77] developed models that take into account the dissolution of the polymer carrier. According to the theory, the polymer chain, at the surface of the system, disentangles (above a critical water concentration) and diffuses into the release medium. The kinetics of the polymer mass loss is controlled by the dissolution rate constant of the polymer and the decreasing with time surface area of the device. Symmetry planes in axial and radial

direction, placed at the center of the matrix, for the water and drug concentration profiles allow the development of an elegant mathematical analysis. Fick's second law of diffusion for cylindrical geometry is used to model both water and drug diffusion. Since both the composition and the dimensions of the device change with time while the diffusion coefficients for both species are considered to be dependent on the water content, the complex partial differential equations obtained are solved numerically. The model has been used successfully to describe the effect of the initial theophylline loading of HPMC-based tablets on the resulting drug release rate.

Recently, a very sophisticated mechanistic model called the *sequential layer* model was presented [78–83]; the model considers inhomogeneous polymer swelling, drug dissolution, polymer dissolution, and water and drug diffusion with nonconstant diffusivities and moving boundary conditions. The raptation theory was used for the description of polymer dissolution, while water and drug diffusion were described using Fick's second law of diffusion. An exponential dependence of the diffusion coefficients on the water content was taken into account. Moving boundaries were considered since the polymer swells, the drug and the polymer dissolve, thereby making the interface matrix/release medium not stationary. The model was applied successfully in the elucidation of the swelling and drug release behavior from HPMC matrices using chlorpheniramine maleate, propranolol HCl, acetaminophen, theophylline, and diclofenac as model drugs.

4.5 Monte Carlo Simulations

In a Monte Carlo simulation we attempt to follow the time evolution of a model that does not proceed in some rigorously predefined fashion, e.g., Newton's equations of motion. Monte Carlo simulations are appropriate for models whose underlying mechanism(s) are of a stochastic nature and their time evolution can be mimicked with a sequence of random numbers, which is generated during the simulation. The repetitive Monte Carlo simulations of the model with different sequences of random numbers yield results that agree within statistical error but are not identical. The goal is to understand the stochastic component of the physical process making use of the perfect control of "experimental" conditions in the computer-simulation experiment, examining every aspect of the system's configuration in detail. Since the mass transport phenomena, e.g., drug diffusion and the chemical processes, e.g., polymer degradation encountered in drug release studies, are random processes, Monte Carlo simulations are used to elucidate the release mechanisms. In the next section we demonstrate the validity of the Higuchi law using Monte Carlo simulations and in the following two sections we focus on the use of Monte Carlo simulations for the description of drug release mechanisms based on Fickian diffusion from Euclidean or fractal spaces. Finally, the last portion of this section deals with Monte Carlo simulations of drug release from bioerodible microparticles.

4.5.1 *Verification of the Higuchi Law*

The presuppositions for the application of the Higuchi law (4.2) have been discussed in Section 4.1. However, it is routinely quoted in the literature without a rigorous proof that only the first 60% of the release curve data should be utilized for a valid application of (4.2). Recently, this constraint has been verified for the Higuchi model using Monte Carlo computer simulations [84] (cf. Appendix B).

To mimic the conditions of the Higuchi model, a one-dimensional matrix of 200 sites has been constructed, Figure 4.4. Each site is labeled with the number of particles it currently hosts. Initially all sites have 10 particles, i.e., the total number n_0 of particles monitored is 2000. Drug molecules move inside the matrix by the mechanism of Fickian diffusion and cannot move to a site unless this site is empty. Thus, the system is expected to behave as if its "concentration" was much higher than its "solubility," which is the basic assumption made in the theoretical derivation of the Higuchi equation. The matrix can leak only from the site at its edge in full analogy with Figure 4.1. The diffusive escape process is simulated by selecting a particle at random and moving it to a randomly selected nearest-neighbor site. If the new site is an empty site, then the move is allowed and the particle is moved to this new site. If the new site is already occupied, the move is rejected. A particle is removed from the lattice as soon as it migrates to the leak site. After each particle move, time is incremented by arbitrary time units, the Monte Carlo microSteps (MCS), during which the movement takes place. One MCS is the smallest time unit in which an event can take place. The increment is chosen to be $1/n\,(t)$, where $n\,(t)$ is the number of particles remaining in the system. This is a typical approach in Monte Carlo simulations. The number of particles that are present inside the cylinder as a function of time is monitored until the cylinder is completely empty of particles. Figure 4.5 shows the simulation results for the first 60% of the release data; the slope of the line is 0.51 very close to the value 0.50 expected by the Higuchi equation.

The simulation results presented in Figure 4.5 provide an indirect proof of the valid use of the first 60% of the release data in line with (4.2). Needless to say, the Monte Carlo simulations in Figure 4.5 do not apply to the diffusion problem associated with the derivation of (4.3).

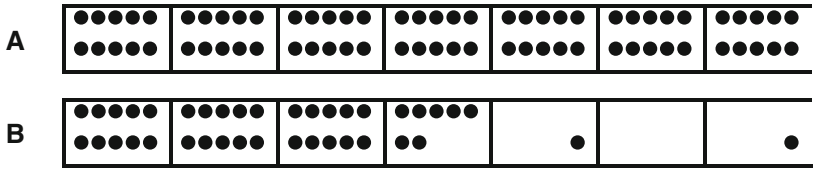

Fig. 4.4 Schematic of a system used to study diffusion under the Higuchi assumptions. (**A**) Initial configuration of the system, (**B**) evolution after time t. Particles are allowed to leak only from the right side of the system. Reprinted from [84] with permission from Springer

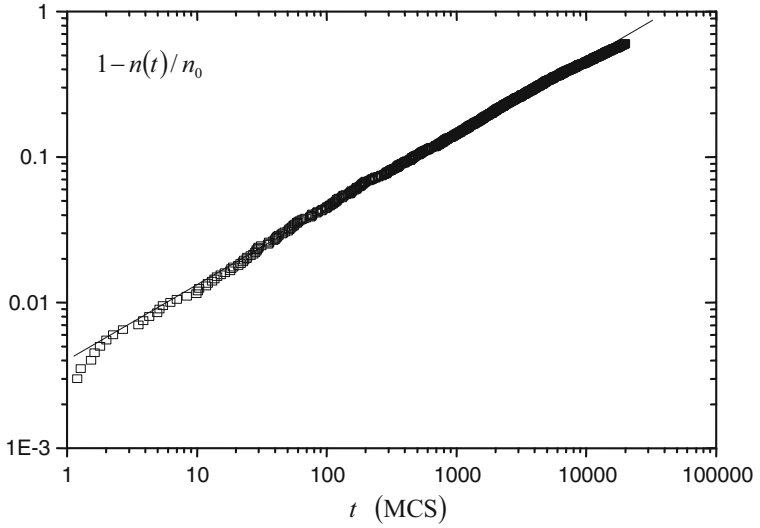

Fig. 4.5 Log-log plot of $1 - n(t)/n_0$ vs. time. Simulation results are indicated as points using the first 60% of the release data. The slope of the fitted line is 0.51 and corresponds to the exponent of the Higuchi equation. The theoretical prediction is 0.50

4.5.2 Drug Release from Homogeneous Cylinders

The general problem that we will focus on in this section is the escape of drug molecules[1] from a cylindrical vessel. Initially, theoretical aspects are presented demonstrating that the Weibull function can describe drug release kinetics from cylinders, assuming that the drug molecules move inside the matrix by a Fickian diffusion mechanism. Subsequently, Monte Carlo simulations will be used to substantiate the theoretical result and provide a link between the Weibull model and the physical kinetics of the release process [84].

4.5.2.1 Theoretical Aspects

A simple approximate solution is sought for the release problem, which can be used to describe release even when interacting particles are present. The particles are assumed to move inside the vessel in a random way. The particle escape rate is expected to be proportional to the number $n(t)$ of particles that exist in the vessel at time t. The rate will also depend on another factor, which will show how "freely" the particles are moving inside the vessel, how easily they can find the exits, how many of these exits there are, etc. This factor is denoted by g. Hence, a differential equation for the escape rate can be written

[1]The terms "drug molecule" and "particle" will be used in this section interchangeably.

$$\dot{n}(t) = -agn(t),$$

where a is a proportionality constant and the negative sign means that $n(t)$ decreases with time. If the factor g is kept constant, it may be included in a and in this case the solution of the previous equation is

$$n(t) = n_0 \exp(-at)$$

using the initial condition $n(0) = n_0$. The last equation is similar to the asymptotic result derived by Fu et al. [72] for pure Fickian diffusion inside a cylinder for long times (cf. Section 4.4).

It stands to reason to assume that the factor g should be a function of time since as time elapses a large number of drug molecules leave the vessel and the rest can move more freely. Thus, in general one can write that $g = g(t)$ and the previous differential equation becomes

$$\dot{n}(t) = -ag(t)n(t). \tag{4.13}$$

A plausible assumption is to consider that $g(t)$ has the form $g(t) \propto t^{-\mu}$.

We are interested in supplying a short-time approximation for the solution of the previous equation. There are two ways to calculate this solution. The direct way is to make a Taylor expansion of the solution. The second, more physical way, is to realize that for short initial time intervals the release rate $\dot{n}(t)$ will be independent of $n(t)$. Thus, the differential equation (4.13) can be approximated by $\dot{n}(t) = -ag(t)$. Both ways lead to the same result.

- For $\mu = 1/2$, (4.13) leads to $n(t) \propto \sqrt{t}$ (as a short-time approximation) exactly as predicted by the Higuchi law.
- For $\mu = 0$ we obtain, again as a short-time approximation, the result $n(t) = n_0 - at$ corresponding to *ballistic* exit (zero-order kinetics).

The above imply that choosing $g(t) = t^{-\mu}$ is quite reasonable. In this case (4.13) will be

$$\dot{n}(t) = -at^{-\mu}n(t).$$

Solving this equation we obtain

$$n(t) = n_0 \exp\left(-at^b\right), \tag{4.14}$$

where $b = 1 - \mu$.

The above reasoning shows that the stretched exponential function (4.14), or Weibull function as it is known, may be considered as an approximate solution of the diffusion equation with a variable diffusion coefficient due to the presence of particle interactions. Of course, it can be used to model release results even when no interaction is present (since this is just a limiting case of particles that are weakly interacting).

It is clear that it cannot be proven that the Weibull function is the best choice of approximating the release results. There are infinitely many choices of the form $g(t)$ and some of them may be better than the Weibull equation. This reasoning merely indicates that the Weibull form will probably be a good choice. The simulation results below show that it is indeed a good choice. The above reasoning is quite important since it provides a physical model that justifies the use of the Weibull function in order to fit experimental release data.

4.5.2.2 Simulations

A brief outline of the Monte Carlo techniques used for the problem of drug release from cylinders is described in Appendix B. The results obtained for cylinders of different dimensions are shown in Figure 4.6. In all cases it is possible to achieve a quite accurate fitting of the simulation results for $n(t)$ using the Weibull function [84]. It turns out that the exponent b takes values in the range 0.69 to 0.75. Figure 4.7 shows that the fitting is very accurate especially at the beginning, and it remains quite good until all of the drug molecules are released. The number of particles that have escaped from the matrix is equal to

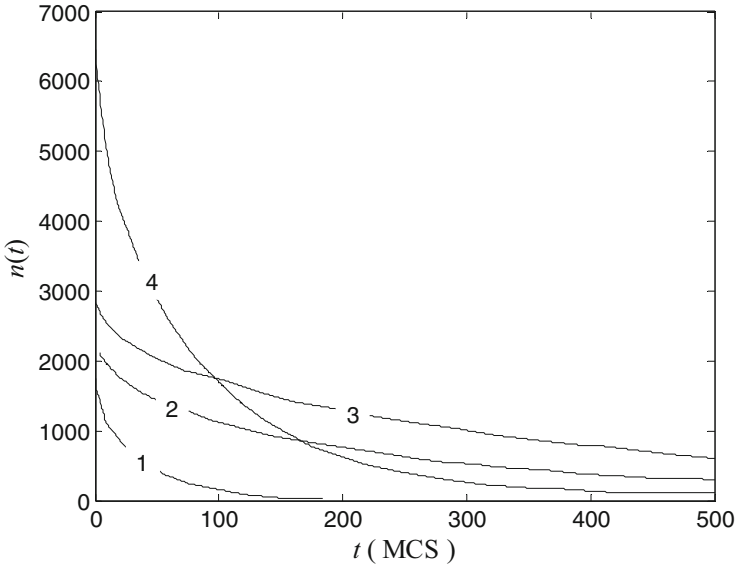

Fig. 4.6 Number of particles inside a cylinder as a function of time. (**1**) Cylinder with height of 31 sites and diameter 16 sites. Number of drug molecules $n_0 = 1750$. (**2**) Cylinder with height 7 sites and diameter 31 sites. Number of drug molecules $n_0 = 2146$. (**3**) Cylinder with height 5 sites and diameter 41 sites. Number of drug molecules $n_0 = 2843$. (**4**) Cylinder with height 51 sites and diameter 21 sites. Number of drug molecules $n_0 = 6452$

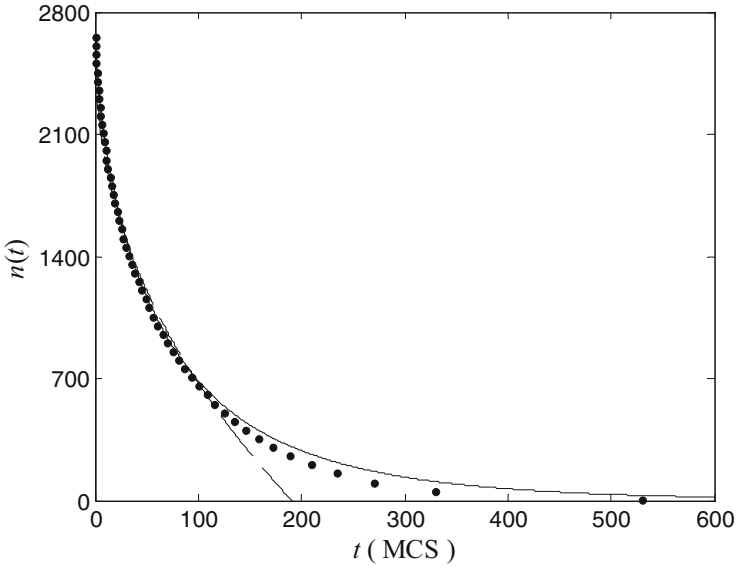

Fig. 4.7 Number of particles inside a cylinder as a function of time with initial number of drug molecules $n_0 = 2657$. Simulation for cylinder with height 21 sites and diameter 21 sites (*dotted line*). Plot of curve $n(t) = 2657 \exp\left(-0.049t^{0.72}\right)$, Weibull model fitting (*solid line*). Plot of curve $n(t) = 2657\left(1 - 0.094t^{0.45}\right)$, power-law fitting (*dashed line*)

$$\tilde{n}(t) = n_0 - n(t) = n_0\left[1 - \exp\left(-at^b\right)\right], \tag{4.15}$$

where a and b are parameters that have to be experimentally determined.

Ritger and Peppas [67, 68] have shown that the power law (4.11) describes accurately the first 60% of the release data. It is easy to show that the two models (4.11) and (4.14) coincide for small values of t. Note that $\tilde{n}(t)/n_0$ is directly linked to $q(t)/q_\infty$. From the Taylor expansion of $\exp(-\chi)$, we can say that for small values of χ we have $\exp(-\chi) \approx 1 - \chi$. From (4.15), setting $\chi = at^b$, one gets

$$\tilde{n}(t)/n_0 = at^b$$

for small values of at^b, which has the same form as the power-law model. For this approximation to hold, the quantity at^b has to be small. This does not mean that t itself must be small. As long as a is small, t may take larger values and the approximation will still be valid.

A comparison of the simulation results and fittings with the Weibull and the power-law model is presented in Figure 4.7. Obviously, the Weibull model describes quite well all release data, while the power law diverges after some time. Of course both models can describe equally well experimental data for the first 60% of the release curve.

4.5.2.3 The Physical Connection Between a, b and the System Geometry

The parameters a and b are somehow connected to the geometry and size of the matrix that contains the particles. This connection was investigated by performing release simulations for several cylinder sizes and for several initial drug concentrations [84]. The Weibull function was fitted to the simulated data to obtain estimates for a and b. If one denotes by N_{leak} the number of leak sites and by N_{tot} the total number of sites, in the continuum limit the ratio $N_{\text{leak}}/N_{\text{tot}}$ is proportional to the leak surface of the system. Plots of a vs. $N_{\text{leak}}/N_{\text{tot}}$ (not shown) were found to be linear and independent of the initial drug concentration; this implies that a is proportional to the specific leak surface, i.e., the surface to volume ratio. The slopes of the straight lines were found to be in the range $0.26 - 0.30$ [84]. The value of the slope can be related to the mathematical model presented in the theoretical section since the number of particles escaping at time dt was assumed to be proportional to $an(t)$; thus, the simulation results can be summarized as $an(t) = 0.28\,(N_{\text{leak}}/N_{\text{tot}})\,n(t)$. Assuming a uniform distribution of particles, $N_{\text{leak}}/N_{\text{tot}}$ is the probability that a particle is at a site that is just one step from the exit. Accordingly, $(N_{\text{leak}}/N_{\text{tot}})\,n(t)$ is the mean number of particles that are able to escape at a given instant of time. Since there are 6 neighboring sites in the three-dimensional space, the probability for a particle to make the escaping step is $1/6$ (≈ 0.17). It is quite close to the 0.28 value of the simulation. The difference is due to the fact that after some time, the distribution of particles is no longer uniform. There are more empty cells near the exits than inside, so the mean number of particles that are able to escape at a given instant is rather less than $(N_{\text{leak}}/N_{\text{tot}})\,n(t)$. This explains the higher value of the slope.

The plot of b values obtained from release simulations for several cylinder sizes and initial drug concentrations vs. $N_{\text{leak}}/N_{\text{tot}}$ (not shown) was also linear [84] with a slope practically independent of the initial concentration, $b = 0.65 + 0.4\,(N_{\text{leak}}/N_{\text{tot}})$. There are two terms contributing to b; one depends on $N_{\text{leak}}/N_{\text{tot}}$ and the other does not. Actually b is expected to be proportional to the specific surface, since a high specific surface means that there are a lot of exits, so finding an exit is easier. The constant term depends on the ability of the particles to move inside the matrix, the interaction between the particles, etc. The linear relationship yields the value of $b = 0.69$ when the exits cover the entire surface of the cylinder ($N_{\text{leak}} = N_{\text{tot}}$).

4.5.3 Release from Fractal Matrices

Apart from the classical mechanisms of release, e.g., Fickian diffusion from a homogeneous release device (cf. Sections 4.5.1 and 4.5.2) or Case II release there are also other possibilities. For example, the gastrointestinal fluids can penetrate the release device as it is immersed in the gastrointestinal tract fluids, creating areas of high diffusivity. Thus, the drug molecules can escape from the release device

through diffusion from these high diffusivity "channels." Now, the dominant release mechanism is diffusion, but in a complex disordered medium. The same is true when the polymer inside the release device is assuming a configuration resembling a disordered medium. This is a model proposed for HPMC matrices [85]. Several diffusion properties have to be modified when we move from Euclidean space to fractal and disordered media.

4.5.3.1 The Pioneering Work of Bunde et al.

The problem of the release rate from devices with fractal geometry was first studied by Bunde et al. [86]. This study was based on a percolation fractal-cluster at the critical point, assuming cyclic boundary conditions, embedded on a two-dimensional square lattice. The concentration of open sites is known to be approximately $p = 0.593$ (cf. Section 1.7). The fractal dimension of the percolation fractal is known to be $91/48$. The simulation starts with a known initial drug concentration $c_0 = 0.5$ and with randomly distributed drug molecules inside the fractal matrix. The drug molecules move inside the fractal matrix by the mechanism of diffusion. Excluded volume interactions between the particles, meaning that two molecules cannot occupy the same site at the same time, were also assumed. The matrix can leak from the intersection of the percolation fractal with the boundaries of the square box where it is embedded. Bunde et al. [86] specifically reported that the release rate of drug in a fractal medium follows a power law and justified their finding as follows: "the nature of drug release drastically depends on the dimension of the matrix and is different depending on whether the matrix is a normal Euclidean space or a fractal material such as a polymer, corresponding to the fact that the basic laws of physics are quite different in a fractal environment."

4.5.3.2 Can the Power Law Describe the "Entire" Release Curve?

Based on the findings of Bunde et al. [86], one can also conceive that the entire, classical % release vs. time curves from devices of fractal geometry should also follow a power law with (a different) characteristic exponent. Although the power law has been extensively used for the description of the initial 60% of the release data, it has also been shown that the power law can describe the entire drug release profile of several experimental data [71]. Typical examples of fittings of (4.11) to experimental data of drug release from HPMC matrices along with the estimates obtained for k and λ are shown in Figures 4.8, 4.9, and 4.10 [71]. In all cases, the entire release profile was analyzed and the fitting results were very good. All these experimental results were explained [71] on the basis of the Bunde et al. [86] findings. However, it will be shown below that the conclusion that the release rate follows a power law is accurate only for infinite problems. For problems in which the finite size is inherent, as happens to be the case in drug release studies, a power law is valid only in the initial stages of the release process.

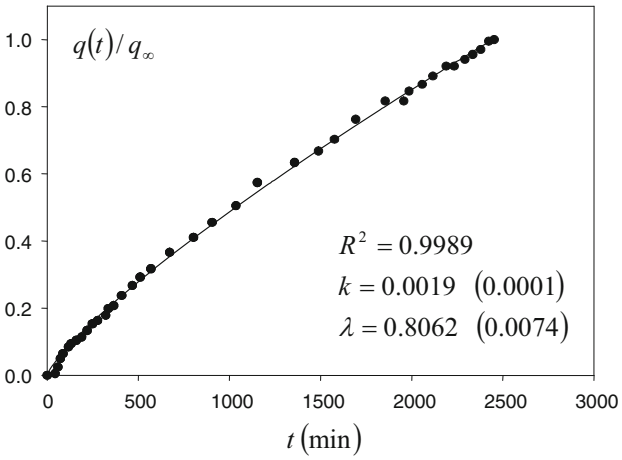

Fig. 4.8 Fitting of (4.11) to the entire set of fluoresceine release data from HPMC matrices [87]

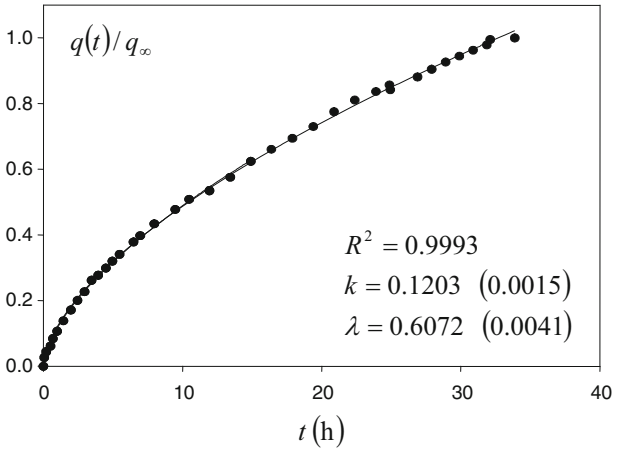

Fig. 4.9 Fitting of (4.11) to the entire set of buflomedil pyridoxal release data from HPMC matrices [88]

4.5.3.3 The Weibull Function Describes Drug Release from Fractal Matrices

Kosmidis et al. [89] reexamined the random release of particles from fractal polymer matrices using the percolation cluster at the critical point, Figure 4.11, following the same procedure as proposed by Bunde et al. [86]. The intent of the study was to derive the details of the release problem, which can be used to describe release when particles escape not from the entire boundary but just from a portion of the boundary of the release device under different interactions between the particles that are present.

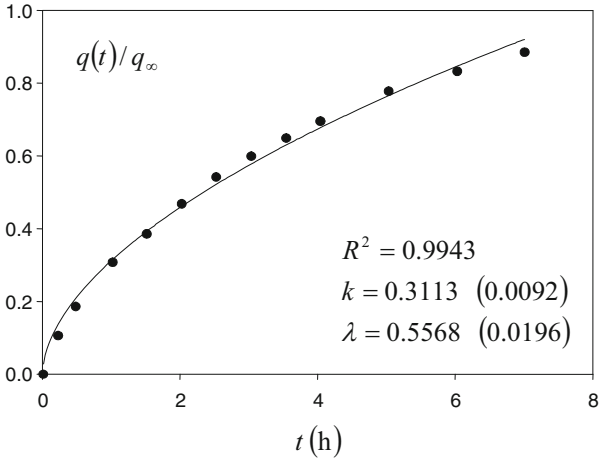

Fig. 4.10 A typical example of fitting (4.11) to chlorpheniramine maleate release data from HPMC K15M matrix tablets (tablet height 4 mm; tablet radius ratio 1 : 1) [83]

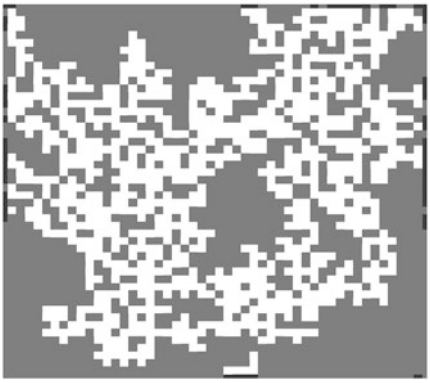

Fig. 4.11 A percolation fractal embedded on a 2-dimensional square lattice of size 50×50. Cyclic boundary conditions were used. We observe, especially on the boundaries, that there are some small isolated clusters, but these are not isolated since they are actually part of the largest cluster because of the cyclic boundary conditions. Exits (release sites) are marked in dark gray, while all lighter gray areas are blocked areas. Reprinted from [89] with permission from American Institute of Physics

The release problem can be seen as a study of the kinetic reaction $A + B \rightarrow B$ where the A particles are mobile, the B particles are static, and the scheme describes the well-known trapping problem [90]. For the case of a Euclidean matrix the entire boundary (i.e., the periphery) is made of the trap sites, while for the present case of a fractal matrix only the portions of the boundary that are part of the fractal cluster constitute the trap sites, Figure 4.11. The difference between the release problem and the general trapping problem is that in release, the traps are not randomly distributed

inside the medium but are located only at the medium boundaries. This difference has an important impact in real problems for two reasons:

- Segregation is known to play an important role in diffusion in disordered media (cf. Section 2.5.1). In the release problem the traps are *segregated* from the beginning, so one expects to observe important effects related to this segregation.
- The problem is inherently a finite-size problem. Results that otherwise would be considered as finite-size effects and should be neglected are in this case essential. At the limit of infinite volume there will be no release at all. Bunde et al. [86] found a power law also for the case of trapping in a model with a trap in the middle of the system, i.e., a classical trapping problem. In such a case, which is different from the model examined here, it is meaningful to talk about finite-size effects. In contrast, release from the surface of an infinite medium is impossible.

The fractal kinetics treatment of the release problem goes as follows [89]. The number of particles present in the system (vessel) at time t is $n(t)$. Thus, the particle escape rate will be proportional to the fraction g of particles that are able to reach an exit in a time interval dt, i.e., the number of particles that are sufficiently close to an exit. Initially, all molecules are homogeneously distributed over the percolation cluster. Later, due to the fractal geometry of the release system segregation effects will become important [17]. Accordingly, g will be a function of time, so that $g(t)$ will be used to describe the effects of segregation (generation of depletion zones), which is known to play an important role when the medium is disordered instead of homogeneous [17].

We thus expect a differential equation of the form of (4.13) to hold, where a is a proportionality constant, $g(t)\,n(t)$ denotes the number of particles that are able to reach an exit in a time interval dt, and the negative sign denotes that $n(t)$ decreases with time. This is a kinetic equation for an $A + B \rightarrow B$ reaction. The constant trap concentration $[B]$ has been absorbed in the proportionality constant a. The basic assumption of fractal kinetics [17] is that $g(t)$ has the form $g(t) \propto t^{-\mu}$. In this case, the solution is supplied by (4.14).

The form of this equation is a stretched exponential. In cases in which a system can be considered as infinite (for example, release from percolation fractals from an arbitrary site located at the middle of the volume) then the number of particles $n(t)$ inside the system is practically unchanged. Treating $n(t)$ as constant and letting $g(t) \propto t^{-\mu}$ in the right-hand side of (4.13) will lead to a power law for the quantity $\dot{n}(t)$. Since most physical problems belong to this class it is widely believed that the release rate from fractal matrices follows a power law. In the case of release from the periphery and if we want to study the system until all particles have escaped, as is often the case for practical applications, then (4.14) is of practical importance.

The above reasoning shows that the stretched exponential function (4.14), or Weibull function as it is known, may be considered as an approximate solution of the release problem. The advantage of this choice is that it is general enough for the description of drug release from vessels of various shapes, in the presence or

absence of different interactions, by adjusting the values of the parameters a and b. Monte Carlo simulation methods were used to calculate the values of the parameters a and (mainly) the exponent b [89].

4.5.3.4 Simulations

The drug molecules move inside the fractal matrix by the mechanism of diffusion, assuming excluded volume interactions between the particles. The matrix can leak at the intersection of the percolation fractal with the boundaries of the square box where it is embedded, Figure 4.11.

The diffusion process is simulated by selecting a particle at random and moving it to a randomly selected nearest-neighbor site. If the new site is an empty site, then the move is allowed and the particle is moved to this new site. If the new site is already occupied, the move is rejected since excluded volume interactions are assumed. A particle is removed from the lattice as soon as it migrates to a site lying within the leak area. After each particle move, time is incremented. As previously, the increment is chosen to be $1/n\,(t)$, where $n\,(t)$ is the number of particles remaining in the system. This is a typical approach in Monte Carlo simulations, and it is necessary because the number of particles continuously decreases, and thus, the time unit is MCS characterizing the system is the mean time required for all $n\,(t)$ particles present to move one step. The number of particles that are present inside the matrix as a function of time until a fixed number of particles (50 particles) remain in the matrix is monitored. The results are averaged using different initial random configurations over 100 realizations. The release rate $\dot{q}\,(t)$ is calculated by counting the number of particles that diffuse into the leak area in the time interval between t and $t + 1$.

Figure 4.12 shows simulation results (line) for the release of particles from a fractal matrix with initial concentration $c_0 = 0.50$, on a lattice of size 50×50. The simulation stops when more than 90% of the particles have been released from the matrix. This takes about $20,000$ MCS. In the same figure the data by Bunde et al. [86] (symbols), which cover the range $50 - 2,000$ MCS, are included. Because of the limited range examined in that study, the conclusion was reached that the release rate $\dot{q}\,(t)$ is described by a power law, with an exponent value between 0.65 and 0.75 [86]. With the extended range examined, Figure 4.12, this conclusion is not true, since in longer times $\dot{q}\,(t)$ deviates strongly from linearity, as a result of the finiteness of the problem.

In Figure 4.13, $n\,(t)\,/n_0$ is plotted as a function of time for different lattice sizes. The data were fitted with a Weibull function (4.14), where the parameter a ranges from 0.05 to 0.01 and the exponent b from 0.35 to 0.39. It has been shown [84] that (4.14) also holds in the case of release from Euclidean matrices. In that case the value of the exponent b was found to be $b \approx 0.70$.

These results reveal that the same law describes release from both fractal and Euclidean matrices. The release rate is given by the time derivative of (4.14). For early stages of the release, calculating the derivative of (4.14) and performing a Taylor series expansion of the exponential will result in a power law for the release

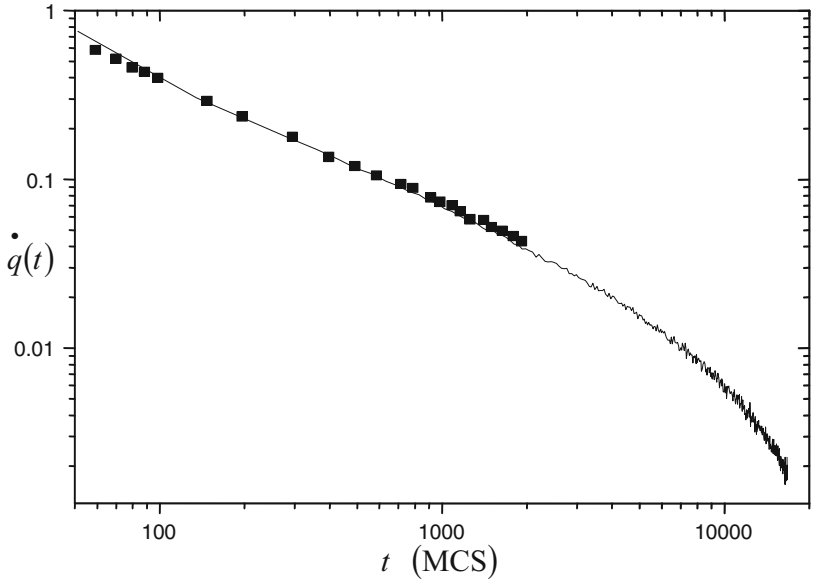

Fig. 4.12 Plot of the release rate $\dot{q}(t)$ vs. time. The lattice size is 50×50 and the initial concentration of particles is $c_0 = 0.50$. Points are the results given in [86], while the line is the result of the simulation in [89]

rate, just as Bunde et al. [86] have observed. If we oversimplify the release problem by treating it as a classical kinetics problem, we would expect a pure exponential function[2] instead of a stretched exponential (Weibull) function. The stretched exponential arises due to the segregation of the particles because of the fractal geometry of the environment. Concerning the release from Euclidean matrices [84], it has been demonstrated that the stretched exponential functional form arises due to the creation of a concentration gradient near the releasing boundaries. Note that although the functional form describing the release is the same in Euclidean and fractal matrices, the value of the exponent b is different, reflecting the slowing down of the diffusion process in a disordered medium. However, these results apparently point to a universal release law given by the Weibull function. The above considerations substantiate the use of the Weibull function as a more general form for drug release studies.

4.6 Discernment of Drug Release Kinetics

In the two previous sections the Weibull function was shown to be successful in describing the entire release profile assuming Fickian diffusion of drug from fractal as well as from Euclidean matrices. Since specific values were found for

[2]The classical kinetics solution is obtained by solving (4.13) in case of $g(t) = 1$.

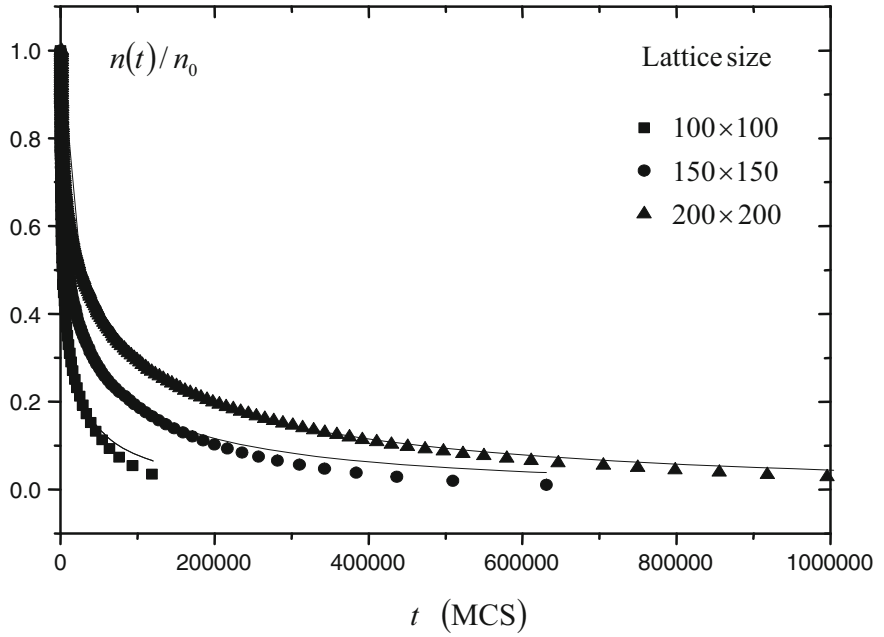

Fig. 4.13 Plot of the number of particles (normalized) remaining in the percolation fractal as a function of time t for lattice sizes 100 × 100, 150 × 150, and 200 × 200. $n(t)$ is the number of particles that remain in the lattice at time t and n_0 is the initial number of particles. Simulation results are represented by points. The *solid lines* represent the results of nonlinear fitting with a Weibull function

the exponent b for each particular case, a methodology based on the fitting results of the Weibull function (4.14) to the entire set of experimental %-release-time data can be formulated for the differentiation of the release kinetics[91]. Basically, successful fittings with estimates for b higher than one (sigmoid curves) rule out the Fickian diffusion of drug from fractal or Euclidean spaces and indicate a complex release mechanism. In contrast, successful fittings with estimates for b lower than one can be interpreted in line with the results of the Monte Carlo simulations of Sections 4.5.2 and 4.5.3. The exponent b of the Weibull function using the entire set of data was associated with the mechanisms of diffusional release as follows:

- $b < 0.35$: Not found in simulation studies [84, 89]. May occur in highly disordered spaces much different from the percolation cluster.
- $b \approx 0.35 - 0.39$: Diffusion in fractal substrate morphologically similar to the percolation cluster [89].
- $0.39 < b < 0.69$: Diffusion in fractal or disordered substrate different from the percolation cluster. These values were not observed in Monte Carlo simulation results [84, 89]. It is, however, plausible to assume this possibility since there has to be a crossover from fractal to Euclidian dimension.

- $b \approx 0.69 - 0.75$: Diffusion in normal Euclidean space [84].
- $0.75 < b < 1$: Diffusion in normal Euclidean substrate with contribution of another release mechanism. In this case, the power law can describe the entire set of data of a combined release mechanism (cf. below).
- $b = 1$: First-order release obeying Fick's first law of diffusion; the rate constant a controls the release kinetics, and the dimensionless solubility–dose ratio determines the final fraction of dose dissolved [92].
- $b > 1$: Sigmoid curve indicative of complex release mechanism. The rate of release increases up to the inflection point and thereafter declines.

When Fickian diffusion in normal Euclidean space is justified, further verification can be obtained from the analysis of 60% of the release data using the power law in accord with the values of the exponent quoted in Table 4.1. Special attention is given below for the values of b in the range $0.75 - 1.0$, which indicate a combined release mechanism. Simulated pseudodata were used to substantiate this argument assuming that the release obeys exclusively Fickian diffusion up to time $t = 90$ (arbitrary units), while for $t > 90$ a Case II transport starts to operate too; this scenario can be modeled using

$$\frac{q(t)}{q_\infty} = 1 - \exp\left(-0.05t^{0.70}\right) + \begin{cases} 0 & \text{for } t \le 90, \\ 0.004\,(t-90)^{0.89} & \text{for } t > 90. \end{cases} \tag{4.16}$$

Also, the following equation was used to simulate concurrent release mechanisms of Fickian diffusion and Case II transport throughout the release process:

$$\frac{q(t)}{q_\infty} = 1 - \exp\left(-0.05t^{0.70}\right) + 0.004t^{0.89}. \tag{4.17}$$

Pseudodata generated from (4.16) and (4.17) are plotted in Figure 4.14 along with the fitted functions

$$y(t) = 0.0652t^{0.5351} \text{ and } y(t) = 0.0787t^{0.5440}.$$

The nice fittings of the previous functions to the release data generated from (4.16) and (4.17), respectively, verify the argument that the power law can describe the entire set of release data following combined release mechanisms. In this context, the experimental data reported in Figures 4.8 to 4.10 and the nice fittings of the power-law equation to the entire set of these data can be reinterpreted as a combined release mechanism, i.e., Fickian diffusion and a Case II transport.

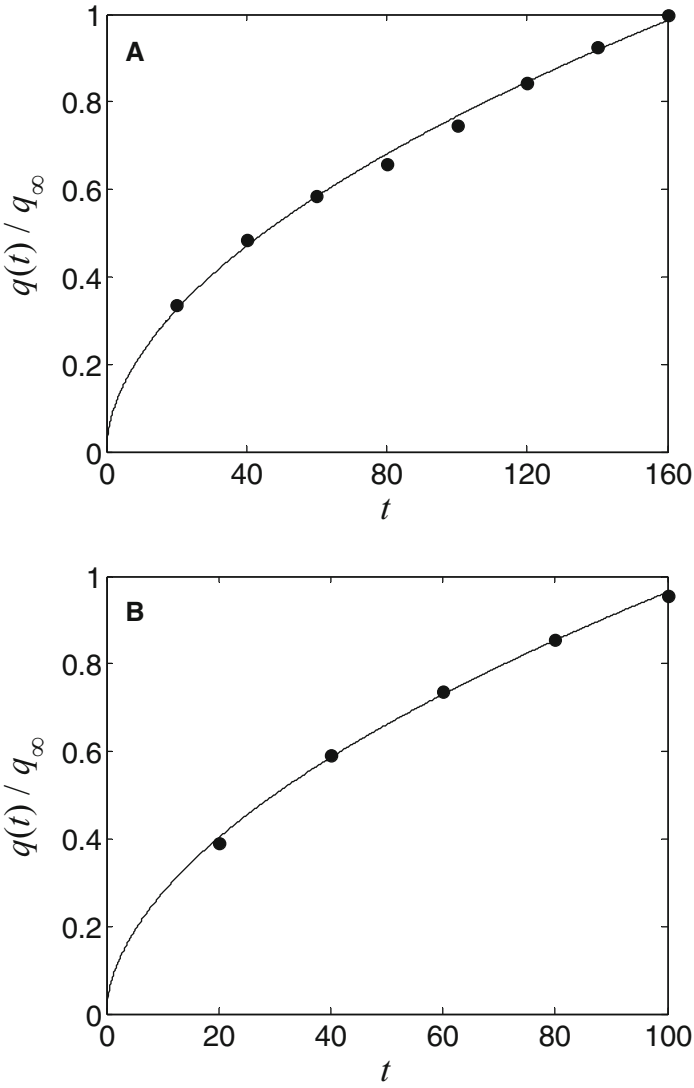

Fig. 4.14 (**A**) Points are simulation data produced using (4.16). The *solid line* is the fitting of the power law (4.11) to data. Best-fitting parameters are $k = 0.0652$ for the proportionality constant and $\lambda = 0.5351$ for the exponent. (**B**) Points are simulation data produced using (4.17). The *solid line* is the fitting of the power law (4.11) to data. Best-fitting parameters are $k = 0.0787$ for the proportionality constant and $\lambda = 0.5440$ for the exponent. Time is expressed in arbitrary units

4.7 Release from Bioerodible Microparticles

In bioerodible drug delivery systems various physicochemical processes take place upon contact of the device with the release medium. Apart from the classical physical mass transport phenomena (water imbibition into the system, drug dissolution, diffusion of the drug, creation of water-filled pores) chemical reactions (polymer degradation, breakdown of the polymeric structure once the system becomes unstable upon erosion) occur during drug release.

The mathematical model developed by Siepmann et al. [93] utilizes Monte Carlo techniques to simulate both the degradation of the ester bonds of the polymer poly-lactic-co-glycolic acid (PLGA) and the polymer's erosion (cleavage of the polymer chains throughout the PLGA matrix). Both phenomena are considered random, and the lifetime of the pixel representing the polymer's degradation is calculated as a function of a random variable obeying a Poisson distribution. The modeling of the physical processes (dissolution and diffusion) takes into account the increase of porosity of the matrix with time because of the polymer's erosion. This information is derived from the Monte Carlo simulations of the polymer's degradation–erosion and allows the calculation of the time- and position-dependent axial and radial diffusivities of the drug. Further, the diffusional mass transport processes are described using Fick's second law with spatially and temporally dependent diffusion coefficients. The numerical solution of the partial differential equation describing the kinetics of the three successive phases of drug release (initial burst, zero-order- and second rapid release) was found to be in agreement with the experimental release data of 5-fluorouracil loaded PLGA microparticles, Figure 4.15 [93]. This model has been further used to investigate the effect of the size of the biodegradable microparticles on the release rate of 5-fluorouracil [94].

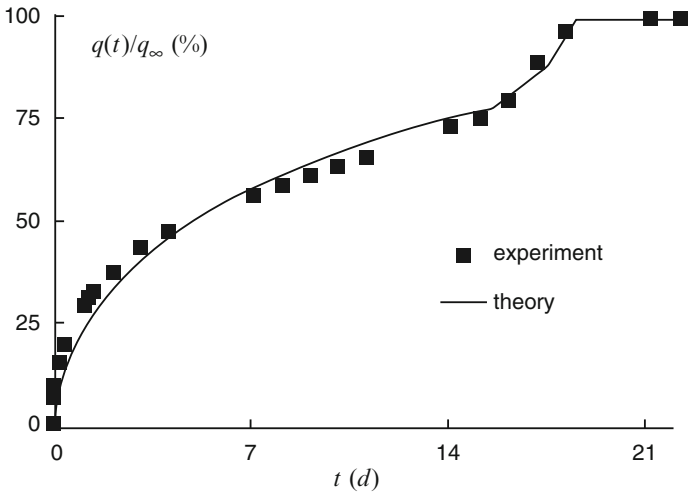

Fig. 4.15 Triphasic drug release kinetics from PLGA-based microparticles in phosphate buffer pH 7.4: experimental data (*symbols*) and fitted theory (*curve*). Reprinted from [93] with permission from Springer

4.8 Dynamic Aspects in Drug Release

Although the development of controlled drug delivery systems is usually based on the simple notion "a constant delivery is optimal," there are well-known exceptions. For example, drug administration in a periodic, pulsed manner is desirable for endogenous compounds, e.g., hormones [95]. The most classical example is the administration of insulin to diabetic patients in order to maintain blood glucose levels at an approximately constant level [96]. In reality, the pancreas behaves as a feedback controller, which changes its output with time in response to food intake or changes in metabolic activity. Hence, the delivery system should not simply maintain insulin levels within an acceptable physiological range to counterbalance the failure of the patient's pancreas to secrete sufficient insulin, but it should also mimic the normal pancreas's feedback controlling function. In other words, the delivery system should secrete insulin according to the (bio)sensed glucose levels in an automatic, periodic manner. These two steps, sensing and delivery, are the basic features of all self-regulated delivery systems regardless the variable, e.g., glucose, temperature, pressure, that is monitored to control the delivery of a pharmacological agent [97].

Since all these systems behave like autonomous oscillators fueled either directly or indirectly by the variable monitored, the factors involved in the production of pulsatile oscillations have been studied thoroughly. One of the most studied means for driving the periodic delivery of drugs is the utilization of chemical pH oscillators [98, 100, 101]. It was demonstrated that periodic drug delivery could be achieved as a result of the effect of pH on the permeability of acidic or basic drugs through lipophilic membranes. The model system of Giannos et al. [100] comprises a thin ethylene vinyl-acetate copolymer membrane separating a sink from an iodate-thiosulfate-sulfite pH oscillator compartment into which drugs like nicotine or benzoic acid are introduced. In the work of Misra and Siegel [98, 101] a model system consisting of the bromate-sulfite-marble pH oscillator in a continuously stirred tank reactor is used, along with acidic drugs of varying concentration. Figure 4.16 provides a schematic for the periodic flux of a drug through the membrane according to the pH oscillations. In one of the studies, Misra and Siegel [98] provided evidence that low concentrations of acidic drugs can attenuate and ultimately quench chemical pH oscillators by a simple buffering mechanism. In the second study, Misra and Siegel [101] demonstrated that multiple, periodic pulses of drug flux across the membrane can be achieved when the concentration of the drug is sufficiently low.

Another approach for periodically modulated drug release is based on an enzyme–hydrogel system, which, due to negative chemomechanical feedback instability, swells and de-swells regularly in the presence of a constant glucose level [102]. The enzyme glucose oxidase catalyses the conversion of glucose to gluconate and hydrogen ions; the latter affect the permeability of the poly(N-isopropylacrylamide-co-methacrylic acid) hydrogel membrane to glucose since the hydrogel swells with increasing pH and de-swells with decreasing pH, Figure 4.17. This system has been studied extensively from a dynamic point of view [99, 103].

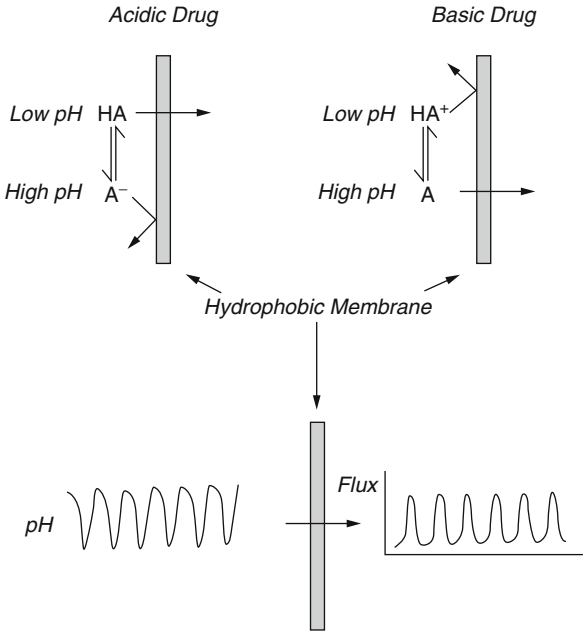

Fig. 4.16 Illustration of conversion of pH oscillations to oscillations in drug flux across a lipophilic membrane. Reprinted from [98] with permission from Wiley–Liss Inc., a subsidiary of John Wiley and Sons, Inc

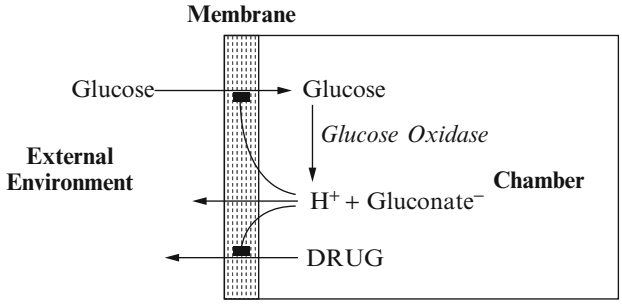

Fig. 4.17 Schematic of pulsating drug delivery device based on feedback inhibition of glucose transport to glucose oxidase through a hydrogel membrane. Changes in permeability to glucose are accompanied by modulation of drug permeability. Reprinted from [99] with permission from American Institute of Physics

It was found that the model allows, depending on system parameters and external substrate concentration, two separate single steady states, double steady state, and permanently alternating oscillatory behavior.